Pharmacological modulation of Acid-Sensing Ion Channels 1a and 3 by amiloride and 2-guanidine-4-methylquinazoline (GMQ)

Thomas Besson, Eric Lingueglia, Miguel Salinas

Pharmacological modulation of Acid-Sensing Ion Channels 1a and 3 by amiloride and 2-guanidine-4-methylquinazoline (GMQ)

Thomas Besson[1,2] , Eric Lingueglia[1,2*#] and Miguel Salinas[1,2*#]

[1]Université Côte d'Azur, CNRS, IPMC, France

[2]LabEx Ion Channel Science and Therapeutics, IPMC, France

 # Equivalent last authors

***Address for correspondence**

Drs Miguel SALINAS and Eric LINGUEGLIA : CNRS, Institut de Pharmacologie Moléculaire et Cellulaire, UMR7275, 06560 Valbonne, France Tel.: 33 4 93 95 34 23; Fax: 33 4 93 95 77 08; E-mail: lingueglia@ipmc.cnrs.fr and salinas@ipmc.cnrs.fr.

Highlights

• First direct comparison of the effect of amiloride (AMI) and GMQ on ASICs

• Gating regulation by AMI and GMQ depends on the nature of the extracellular domain

• The transmembrane/cytosolic domains modulate the pharmacological regulation of ASICs

• Additive effect of AMI and GMQ fits well with a common unique binding site

• Mechanisms of gating regulation by GMQ & PcTx1, but not mambalgin, partially overlap

Abstract

Acid-Sensing Ion Channels (ASICs) are cation channels activated by extracellular acidification that emerge as potential pharmacological targets in pain and other neurological disorders. Here, we compare the pharmacological modulation of ASIC1a and ASIC3 channels by amiloride and 2-guanidine-4-methylquinazoline (GMQ), two compounds commonly used for their *in vitro* and *in vivo* investigation. We analyzed the effect of amiloride on the pH-dependent activation and inactivation, the relative influence of the extracellular domain and the transmembrane/cytosolic domains on the effect of amiloride and GMQ using chimeras between ASIC1a and ASIC3, and how these compounds potentiate the physiologically relevant ASIC3 sustained window current. We showed that amiloride and GMQ shift the pH-dependent activation and inactivation in the same directions, which depend on the channel, and that their effects rely on the nature of the extracellular domain but can be indirectly modulated in their amplitude by the transmembrane/cytosolic domains. The extracellular domain explains the pharmacological potentiating effect of amiloride and GMQ on the window current in ASIC3, and why these compounds failed to generate a window current in ASIC1a. Amiloride and GMQ have similar and purely additive effects suggesting that they act through a common unique binding site different from acidic pockets. Finally, a simple cycle analysis using GMQ that targets the nonproton ligand-sensor, and two peptide inhibitors of ASIC1a targeting the acidic

pockets (PcTx1 and mambalgin-1), shows overlap between the mechanisms by which GMQ and PcTx1 modify inactivation and suggests shared mechanisms of regulation of the pH-dependent inactivation of ASIC1a between these two regions.

Keywords: Acid-Sensing Ion Channel (ASIC); pH-dependent gating; GMQ; amiloride; mambalgin; PcTx1.

Chemical compounds studied in this article: Amiloride hydrochloride (PubChem CID: 16230); 1-(4-methylquinazolin-2-yl)guanidine hydrochloride (PubChem CID: 12253739).

Footnotes: The abbreviations used are: ASIC, acid-sensing ion channel; Mamb-1, mambalgin-1; PcTx1, Psalmatoxin-1; (N/TM/C), transmembrane and cytosolic domains of ASIC; ECD, ExtraCellular Domain of ASIC; GMQ, 2-guanidine-4-methylquinazoline; AMI, amiloride.

1. Introduction

Acid-Sensing Ion Channels (ASICs) (Waldmann et al., 1997b) are voltage-independent cation channels activated by extracellular acidification (ASIC1-3) and lipids (ASIC3) (Marra et al., 2016). They are widely expressed in the peripheral and the central nervous systems, where they are involved in physiological and pathophysiological processes ranging from synaptic plasticity and neuronal injury to nociception and mechanoperception (Meng et al., 2009; Noel et al., 2010; Schuhmacher and Smith, 2016; Wemmie et al., 2013). ASICs appear as interesting pharmacological targets with potential clinical applications in the treatment of pain (Diochot et al., 2012; Mazzuca et al., 2007), psychiatric disorders (Wemmie et al., 2003) stroke and neurodegenerative diseases (Friese et al., 2007; Xiong et al., 2004). Understanding of the

regulations of these channels by pharmacological agents appears therefore to be crucial for their optimal use and for further drug development.

Amiloride is a well-known non-selective inhibitor of ASICs that acts as a non-discriminative low affinity pore-blocker through a binding site into the pore. A paradoxical stimulatory effect on ASIC3 was also described and associated with a possible binding site in the extracellular domain (Adams et al., 1999; Li et al., 2011; Waldmann et al., 1997a; Yagi et al., 2006). Crystallographic data and molecular docking have further suggested binding of amiloride into the acidic pockets (Baconguis et al., 2014; Qadri et al., 2010), although binding into a different nonproton ligand sensing domain that was first identified as the binding site of GMQ (2-guanidine-4-methylquinazoline), a positive modulator of ASIC3 (Yu et al., 2010), has also been proposed (Li et al., 2011). On the other side, PcTx1 and mambalgin-1 are peptides specifically targeting ASIC channels to relieve pain (Diochot et al., 2012; Mazzuca et al., 2007). Both peptides binds into the acidic pocket (Baconguis and Gouaux, 2012; Mourier et al., 2016; Salinas et al., 2014; Salinas et al., 2006; Schroeder et al., 2014) and are able to inhibit (and sometimes to potentiate) the ASIC currents by stabilizing either the inactivated state or the closed state (Chen et al., 2005; Salinas et al., 2014).

Structure-function relationship studies have shown that protons bind to different regions of the extracellular domain of ASIC channels including three acidic pockets formed at the three interfaces of the functional trimeric channel (also named pH-sensors) (Baconguis and Gouaux, 2012), and several amino acids outside of these pockets in the β-sheet region composing the Palm domain (Della Vecchia et al., 2013; Krauson et al., 2013; Liechti et al., 2010; Paukert et al., 2008; Schuhmacher et al., 2015; Vullo et al., 2017). The binding of protons on these different sites leads to several conformational changes, which are propagated through the flexible Wrist domain, involving the Thumb and the Palm domains, to the transmembrane domains (TM1 and TM2) forming the pore (Gonzales et al., 2009). Pharmacological

modulators like the small molecules GMQ and amiloride, or the peptides PcTx1 and mambalgin-1, are able to interfere with the activation and inactivation of ASIC channels (Alijevic and Kellenberger, 2012; Chen et al., 2006; Diochot et al., 2012; Li et al., 2011; Salinas et al., 2014; Yu et al., 2010). GMQ and amiloride are known to potentiate the sustained window current present in ASIC3, but not in ASIC1a, which results from the overlap between pH-dependent activation and inactivation curves (Yagi et al., 2006; Yu et al., 2010). This sustained current, and its pharmacological regulation, are of particular interest because of its proposed role in non-adapting pain caused by tissue acidosis (Deval and Lingueglia, 2008; Waldmann et al., 1997b; Yagi et al., 2006).

Amiloride and GMQ have been widely used to characterize the *in vitro* and *in vivo* functions of ASICs, but surprisingly, the effects of amiloride on the pH-dependent activation and inactivation of ASIC1a and ASIC3 have, to our knowledge, never been fully investigated. A detailed back-to-back comparison of these two compounds, which have been proposed to share some mechanism of action (Li et al., 2011), had also never been done over a broad range of pHs. We investigated here the pharmacological modulation of ASIC1a and ASIC3 by amiloride and GMQ, including the effect of amiloride on the pH-dependent activation and inactivation, analysis of the cooperativity of their effects (inferring the amiloride binding-site) and of the relative influence of the ECD and (N/TM/C) domains, and of how they potentiate the physiologically relevant ASIC3 sustained window current. We also took advantage of the binding site of amiloride and GMQ that is different from the one of the peptide toxins PcTx1 and mambalgin-1, to explore the overlap between the mechanisms by which they modify activation and inactivation and gain some information on the gating of ASIC channels.

2. Materials and Methods

2.1 Plasmid Constructions and Mutagenesis

The coding sequences of rat ASIC1a, rat ASIC3 (GenBank Accession Number #U94403 and #AF013598, respectively) and the related chimeras and mutant were subcloned into the NheI/NotI restriction sites of the pCI vector (Promega). Chimeras were obtained by recombinant PCR strategies as previously described (Salinas et al., 2006). Chimeras ASIC3ECD1a and ASIC1aECD3 have been fully described in a previous article (Salinas et al., 2009). The flexible Wrist region of ASIC1a and ASIC3 involved in the coupling of the extracellular domain (ECD) to the transmembrane and cytosolic domains (N/TM/C) have been conserved in the complementary chimeras ASIC1aECD3 and ASIC3ECD1a by transferring the ECD region together with the three first amino acids of the upper part of the transmembrane domain 1 and 2 (Supplementary Figures 1A and 2).

2.2 Xenopus Oocyte Preparation, DNA Injection, and Electrophysiology

Animal handling and experiments fully conformed to French regulations and were approved by local governmental veterinary services (authorization number B061525 delivered by the Ministère de l'Agriculture, Direction des services vétérinaires). Animals were anesthetized by exposure for 20 min to a 0.1% solution of 3-aminobenzoic acid ethyl ester (MS-222) (Sigma) buffered at pH 7.4. Oocytes were surgically removed and dissociated with collagenase type IA (Sigma) in the presence of trypsin inhibitor (Sigma), then injected into the nucleus with: 18 nl of pCI-ratASIC1a (1-5 ng/µl) or pCI-ratASIC3 (25 ng/µl) plasmids, or with mutant and chimeras: pCI-ratASIC3-L529A (25 ng/µl), pCI-ratASIC3ECD1a (25 ng/µl) or pCI-ratASIC1aECD3 (25 ng/µl). Oocytes were kept at 19°C in ND96 solution containing 96 mM NaCl, 2 mM KCl, 1.8 mM $CaCl_2$, 2 mM $MgCl_2$, and 5 mM HEPES (pH 7.4 with NaOH) with penicillin (6 µg/ml) and streptomycin (5 µg/ml). ASIC currents were recorded using the two-

electrode voltage-clamp technique with two standard glass microelectrodes (0.5–2.5 mega-ohms) filled with a 3 M KCl, 1–3 days after injection using a manual setup (Dagan TEV 200 amplifier, Dagan Corp.). Oocytes were clamped at -50 mV, and ASIC currents were activated by rapid changes in extracellular pH induced by a microperfusion system. HEPES was replaced by MES (5 mM) in experiments performed using low pH (pH 6.5-4.0). Stimulation, data acquisition, and analysis for manual recordings were performed using pCLAMP 9.2 software (Axon Instruments). All experiments were performed at 19°C in ND96 solution supplemented with 0.05% fatty acid- and globulin-free-bovine serum albumin (Sigma) to prevent nonspecific adsorption of the peptides to tubing and containers. Synthetic mambalgin-1 (Smartox) and PcTx1 (Synprosis/Provepep) were applied 30 s and 1 min before the acid stimulation, respectively, or during the pH pulses as indicated in some protocols. Amiloride (Sigma) and GMQ (Sigma) were applied during the pH pulses (1mM each in ND96 solution from 25 mM stock solutions in water).

3. Theory/calculation

3.1 Simple Cycle Analysis

To determine if two compounds A and B have additive, synergistic or antagonistic effects, a simple cycle analysis has been done by using a new variable that we named Zeta (Z). To determine it, the $pH_{0.5act}$ and $pH_{0.5inact}$ (Table 1), calculated from the pH-dependent curves of activation and inactivation, were used to estimate the proton sensitivity of the activation and inactivation mechanisms. The pH sensitivity change ($\Delta pH_{0.5}$) when going from ASIC alone to ASIC treated by a mix of A+B (inset Fig. 4C,D and 5F) must be the same regardless of the pathway taken, and is described by : ***(V) = (I) + (IV) = (III) + (II)*** with for example: (I)= $\Delta pH_{0.5\rightarrow A} = pH_{0.5A} - pH_{0.5control}$. The variable Zeta was calculated as follow based on the

definition of the Ω variable made in the classical double-mutant cycle analysis approach (Hidalgo and MacKinnon, 1995; Li et al., 2009):

$$\boldsymbol{Z = (IV) - (III) = (II) - (I)} \qquad \textit{Equation 1}$$

$$Z = (pH_{0.5A/B} - pH_{0.5B}) - (pH_{0.5A} - pH_{0.5})$$

$$\boldsymbol{Z = pH_{0.5} + pH_{0.5A/B} - pH_{0.5A} - pH_{0.5B}} \qquad \textit{Equation 2}$$

Zeta can also be developed as follow:

$$Z= pH_{0.5} + pH_{0.5A/B} - pH_{0.5B} - pH_{0.5A} + (pH_{0.5} - pH_{0.5})$$

$$Z= (pH_{0.5A/B} - pH_{0.5}) - (pH_{0.5B} - pH_{0.5}) - (pH_{0.5A} - pH_{0.5})$$

$$\boldsymbol{Z_{A/B}=\Delta pH_{0.5\rightarrow A/B} - \Delta pH_{0.5\rightarrow A} - \Delta pH_{0.5\rightarrow B}}$$

or

$$\boldsymbol{Z = (V) - (I) - (III)} \qquad \textit{Equation 3}$$

Thus, the simple cycle analysis equation corresponds to the difference between the variations of $pH_{0.5}$ induced by a mix of A+B minus the sum of individual effects generated by A and B. Thus, $Z_{A/B}=0$, $Z_{A/B}>0$ or $Z_{A/B}<0$ indicate a pure additive effect, a positive cooperativity, or a negative cooperativity, respectively, between compounds A and B (Mildvan et al., 1992). Note that because cooperativity is interpreted relative to the pH-dependence, and not from the respective effects of compounds A or B, a negative $Z_{A/B}$ value indicates a negative cooperativity because it means that the shift of $pH_{0.5}$ is more acidic (i.e., more protons are necessary) than the theoretical shift deduced from the sum of individual effects.

3.2 Statistical analysis

Data analysis was performed using GraphPad Prism 4.03 software.

The I/Imax values are represented as means ± S.E.M., and the statistical significance of differences between sets of data measured on the same current trace were estimated with

nonparametric, paired t-test, Wilcoxon signed rank test: ^{ns} P>0.05, * P < 0.05; ** P < 0.01; *** P < 0.001.

The $pH_{0.5}$ values are represented as means ± S.E.M., and the statistical significance of differences between sets of data were estimated using the one-way analysis of variance followed by Tukey's multiple comparison test (^{ns} P>0.05, * P < 0.05; ** P < 0.01; *** P < 0.001).

The $\Delta pH_{0.5}$ values are represented as a "difference of means" ± "sum of S.E.M" from the $pH_{0.5}$ composing the $\Delta pH_{0.5}$: $\delta\Delta pH_{0.5}=\delta pH_{0.5control}+\delta pH_{0.5.}$ The $\Delta pH_{0.5}$ is significantly different from zero when the two $pH_{0.5}$ composing this difference are statistically different. When two $\Delta pH_{0.5}$ have the same control conditions, it is possible to estimate their statistical difference by directly comparing the $pH_{0.5}$ of the two tested conditions (^{ns} P>0.05, $^{\delta}$ P < 0.05; $^{\delta\delta}$ P < 0.01; $^{\delta\delta\delta}$ P < 0.001).

The standard error associated with Zeta (δZ) was calculated as: $\delta Z=\delta pH_{0.5}+\delta pH_{0.5A/B}+\delta pH_{0.5A}+\delta pH_{0.5B}$, where the different $\delta pH_{0.5}$ are the standard error associated with $pH_{0.5}$ measurement.

4. Results

4.1 The effects of amiloride and GMQ depend on the extracellular domain of ASICs and can be modulated by the transmembrane/cytosolic domains.

A description of the effect of GMQ on the pH-dependent curves of activation and inactivation was recently published for ASIC1a and ASIC3 (Alijevic and Kellenberger, 2012). The effects of amiloride on the pH-dependent activation and inactivation of the two distant isoforms ASIC1a and ASIC3 (54% amino acid identity) remain however largely unknown. To facilitate the recording of the very small window currents, which represent only around 1% of the peak current for ASIC3 (Supplementary Fig. 1B), we have built the ASIC3-L529A point mutant ($ASIC3^{L/A}$), where a consensus motif for internalization close to the end of the

cytoplasmic carboxy-terminus has been altered. This mutation increases the expression in the *Xenopus* oocyte system without affecting the other biophysical (Supplementary Fig. 1B-D) and pharmacological (Supplementary Fig. 1E-G) properties of ASIC3. Here we showed that both amiloride and GMQ behave very similarly in $ASIC3^{L/A}$ (Fig. 1A,B) by shifting the activation and inactivation curves toward alkaline and acidic pH, respectively (Fig. 1C,D,G and Table 1), and in ASIC1a by shifting the activation and inactivation curves toward acidic pH (Fig. 2A,B,E and Table 1), in good agreement with the data of Alijevic et al for the effect of GMQ (Alijevic and Kellenberger, 2012). However the amplitude for the shift of inactivation by amiloride is lower than with GMQ in $ASIC3^{L/A}$ and even not statistically significant in ASIC1a. Although a smaller effect of amiloride on inactivation is observed, amiloride and GMQ behave similarly on the pH-dependent activation and inactivation but the direction of these effects depends on the channel under consideration.

To quantify the relative contribution of the extracellular domain and the indirect influence of the transmembrane/cytosolic domains (identified here as ECD and N/TM/C, respectively, Supplementary Fig. 1A) in the pharmacological modulation of ASIC1a and ASIC3, we have characterized the complementary chimeras ASIC1aECD3 and ASIC3ECD1a previously described in another context (Salinas et al., 2009). In these chimeras, the Wrist domain connecting the Thumb domain with the upper part of the first transmembrane domain (TM1), and the Palm domain covalently linked to both transmembrane domains, have been conserved to preserve the correct interface and the coupling between the extracellular domain and the rest of the channel during the pH-dependent gating (see Supplementary Figure 1A for a schematic representation of the different domains defining the ASIC structure). In particular, the crucial amino acids that have been described to establish the non-covalent Thumb/TM1 connection (i.e., Tyr71 at the external end of TM1, and Trp287 in the β-turn structure that is part of a Palm−Thumb loop of rat ASIC1a (Li et al., 2009)) are included in our extracellular domain

(Salinas et al., 2009) and are therefore always swapped together (Supplementary Figure 2). Note that the L529A mutation has not been introduced into chimera ASIC3ECD1a, which already displayed a sufficient level of expression in *Xenopus* oocyte.

In chimera ASIC1aECD3, where the extracellular domain of ASIC1a has been swapped by the one of ASIC3, amiloride and GMQ shifts the activation and inactivation curves similarly to ASIC3 (Fig. 1E-G and Table 1) but differently from ASIC1a (Fig. 2A,B and Table 1), suggesting an important role of the ECD3 in the effect of the two guanidine compounds on ASIC3. However, the amplitude of the activation and inactivation shifts is smaller compared with ASIC3, which suggests that amplitudes of these effects are strongly influenced by the nature of the (N/TM/C) domains.

In chimera ASIC3ECD1a, where the extracellular domain of ASIC3 has been swapped by the one of ASIC1a, amiloride and GMQ shifts the activation and inactivation curves similarly to ASIC1a (Fig. 2C-E and Table 1) but differently from ASIC3 (Fig. 1C,D,G and Table 1), suggesting again an important role of the ECD1a in their effect on ASIC1a. However, and contrary to the effect on ASIC3, the activation and inactivation curves are both shifted in the same direction by amiloride and GMQ (Fig. 2C-E). In addition, the amplitude of the activation and inactivation shifts induced by GMQ is similar to the one seen on ASIC1a, which suggests only a weak influence of the (N/TM/C) domains in this case. On the other side, the effect of amiloride is potentiated by the (N/TM/C)3 domains, leading to a significant shift of both activation and inactivation in chimera ASIC3ECD1a compared to ASIC1a (Fig. 2B,D,E).

All together, these data show that the difference in the effects of amiloride and GMQ (i.e., direction of the shift of the curve) observed between ASIC1a and ASIC3 directly depends on the nature of the ECD and that the amplitudes of these effects can be modulated by the nature of transmembrane/cytosolic domains.

4.2 Influence of GMQ and amiloride on the ASIC window current

Amiloride and GMQ modulate the pH-dependent activation and inactivation of ASIC3 in a similar way but with a smaller effect of amiloride on inactivation (Fig. 1G). They strongly increase the sustained window current generated at moderate acidification in ASIC3 by increasing the overlap of the pH-dependent curves of activation and inactivation (Fig. 1 C,D and Fig. 3A,D), but not in ASIC1a (Fig. 2 A,B and Fig. 3B,E). However, amiloride induced a smaller shift of inactivation compared with GMQ (Fig. 1G and Table 1), and also displayed a pore blocker effect (Fig. 1B), which explains the smaller potentiating effect of amiloride on the window current compared with GMQ (Fig. 3A). Amiloride and GMQ are still able to generate a small window current in chimera ASIC1aECD3 (Fig. 3C,F). However, as for ASIC3, the shift of inactivation by amiloride is smaller (Fig. 1G), which explains and is coherent with the smaller window currents compared with GMQ (Fig. 3C). A window current was observed in chimera ASIC3ECD1a (Fig. 3G), which is not potentiated by amiloride and GMQ but only shifted toward more acidic pH (Fig. 2C,D, insets). The shift of the activation and inactivation curves in the same direction by GMQ or amiloride does not increase the overlap of both curves (Fig. 2A,B) and explains why these two compounds are not able to potentiate the window current of ASIC3ECD1a (Fig. 3G) or to induce a window current in ASIC1a (Fig. 3B,E).

Overall, the distinct effects of amiloride and GMQ on the gating of ASIC1a or ASIC3, which depend on the nature of the extracellular domain, are consistent with the fact that both compounds do not allow the generation of a window current in ASIC1a while they lead to a strong potentiation of the one already present in ASIC3.

4.3 The effects of amiloride and GMQ are purely additive

A simple cycle analysis was performed to further explore the mechanism of action of amiloride and GMQ and their possible cooperativity. The Zeta value (see Theory/Calculation)

was calculated to determine if the two modulators have purely additive effects on the pH-dependent activation and inactivation (i.e., a Zeta value close to zero) or if they display a positive- or negative-cooperative effect (i.e., a positive or negative Zeta value). GMQ (1mM) was always able to induce the same acidic shift of the activation and inactivation curves in ASIC1a in the presence or in the absence of amiloride (1mM) ($\Delta pH_{0.5(AMI/GMQ)-AMI}$ =-0.22±0.07 and -0.19±0.03 versus $\Delta pH_{0.5GMQ}$=-0.32±0.04 and -0.17±0.02 for activation and inactivation, respectively; P>0.05; Fig. 4A,E). The simple cycle analysis showed that both molecules have a pure additive effect and therefore no cooperativity during the activation and inactivation processes of ASIC1a ($Z_{act\ GMQ/AMI}$ =0.10±0.11 and $Z_{inact\ GMQ/AMI}$ = -0.02±0.05; Fig. 4F). In $ASIC3^{L/A}$, GMQ (1 mM) was always able to induce an acidic shift of inactivation with or without 1 mM amiloride ($\Delta pH_{0.5(AMI/GMQ)-AMI}$=-0.73±0.04 versus $\Delta pH_{0.5GMQ}$=-0.72±0.02 for inactivation; P>0.05; Fig. 4B,E). A simple cycle analysis indicates a pure additive effect of amiloride and GMQ for inactivation ($Z_{inact\ GMQ/AMI}$=-0.02±0.07; Fig. 4F). The procedure has been slightly modified to check the effect of amiloride and GMQ on the activation of $ASIC3^{L/A}$ because of possible experimental limitations to measure the effect of GMQ on activation at a concentration of 1mM and at pH values above 8.0 (such alkaline pHs were not used in experiments described above with ASIC1a). Indeed, the pKa of GMQ and amiloride (8.5 and 8.7, respectively) indicates that a great proportion of these molecules must be deprotonated at pH~8.0. Moreover, several important residues in rat ASIC3 close to the nonproton ligand sensor (the paired Glu416/Glu79 residues and Arg80 residue (Li et al., 2011; Liechti et al., 2010) could also be deprotonated at pH~8.0, which is the theoretical $pH_{0.5}$ value necessary to reach a $Z_{acti\ GMQ(1mM)/AMI(1mM)}$ close to zero. The $pH_{0.5act}$ of ASIC3 in the presence of both 1 mM GMQ and 1 mM amiloride is 7.24±0.03 (Fig. 4B and Table 1), a value very close to calculated pKa of the key residue Glu416 in ASIC3 (estimated to 7.2; (Liechti et al., 2010). To avoid this artifact on the activation mechanism due to deprotonation at alkaline pH of GMQ, amiloride

and/or key residues in ASIC3, a simple cycle analysis was therefore achieved with a two-fold decreased concentration of GMQ and amiloride to limit the shift of $pH_{0.5}$ ($\Delta pH_{0.5(AMI/GMQ)-AMI(0.5mM)}$=-0.50±0.06 versus $\Delta pH_{0.5GMQ(0.5mM)}$=-0.46±0.06 for activation; P>0.05; Fig. 4C,E). In these conditions, GMQ and amiloride had a pure additive effect ($Z_{act\ GMQ/AMI}$=-0.03±0.12; Fig. 4F). Simple cycle analysis thus indicates a pure additive effect of amiloride and GMQ for inactivation and activation of $ASIC3^{L/A}$ (Fig. 4F). Both mechanisms are therefore non-cooperative, as for ASIC1a. Interestingly, the effect of GMQ on $ASIC3^{L/A}$ was also purely additive on itself ($Z_{act\ GMQ\ 0.5mM/GMQ\ 0.5mM}$ = 0.02±0.15; Fig. 4D,F) contrary to the strong cooperativity seen with protons (Bonifacio et al., 2014).

4.4 Comparison of the mechanism of action in ASIC1a of GMQ and of the two peptides PcTx1 and mambalgin-1

We have shown that amiloride and GMQ have a similar regulatory mechanism, which depends on the extracellular domain and probably involves the same binding site different from the acidic pockets (Yu et al., 2010; Yu et al., 2011). On the other side, PcTx1 and mambalgin-1, two venom-derived peptide modulators of ASIC1a, specifically bind into the acidic pockets (Baconguis and Gouaux, 2012; Salinas et al., 2014; Salinas et al., 2006; Schroeder et al., 2014). PcTx1 principally induces a shift of the inactivation curve of ASIC1a toward alkaline pH (Chen et al., 2005 and Fig. 5A), meaning that this peptide inhibits the channel by stabilizing the inactivated state (Chen et al., 2005) even if PcTx1 is also able to slightly stabilize the open state at the same time. Inversely, mambalgin-1 principally induces an acidic shift of the activation curves of ASIC1a (Fig. 5B) through stabilization of the closed state (Diochot et al., 2012). We therefore took advantage of the fact that amiloride and GMQ on one side, and the blocking peptides on the other side target different sites in the ECD of ASIC1a to design a set of experiments to compare the mechanisms of action of GMQ and PcTx1 or mambalgin-1, and to

evaluate their possible overlap. Only GMQ was used because it induces an effect sufficiently strong to be measurable compared with amiloride (see Fig. 2A,B). GMQ was able to generate an acidic shift of the pH-dependent curves of activation and inactivation of ASIC1a in the presence of PcTx1 (Fig. 5C,E) or mambalgin-1 (Fig. 5D,E). A simple cycle analysis (Fig. 5F) showed that the effects of GMQ and PcTx1 or mambalgin-1 were purely additive on the pH-dependent activation ($Z_{act\ GMQ/PcTx1}$ = -0.02±0.09 and $Z_{act\ GMQ/mamb1}$ = 0.04±0.10), supporting two independent mechanisms for the regulation of activation by GMQ and these two peptides. The negative cooperativity found for the pH-dependent inactivation in the presence of PcTx1 ($Z_{inact\ GMQ/PcTx1}$ = -0.22±0.04) but not mambalgin-1 ($Z_{inact\ GMQ/mamb1}$ = 0.01±0.04; Fig. 5F) indicates that the pH-dependent regulations of inactivation by GMQ and PcTx1 share an overlapping mechanism while the regulations by GMQ and mambalgin-1 involve independent mechanisms.

5. Discussion

We have investigated here the pharmacological modulation of ASIC1a and ASIC3 by amiloride and GMQ. By quantifying the effects of these two pharmacological agents that are widely used to characterize the *in vitro* and *in vivo* functions of ASIC channels, this work will probably provide some clues for further optimization of the experimental conditions using these compounds. The gating regulation by these two compounds is mostly similar and depends on the channel under consideration, and more specifically on the nature of the extracellular domain. They evoke, via the ECD1, an acidic shift of both the pH-dependent activation and inactivation and, via the ECD3, an alkaline and acidic shift of the pH-dependent activation and inactivation, respectively. The N/TM/C domains modulate amplitude of these effects. It explains why amiloride and GMQ potentiate the sustained window current in ASIC3 but failed to generate any in ASIC1a. Their additive effect fits well with a common unique binding site

different from the acidic pockets. This difference has been used to examined the overlap in ASIC1a between the inhibitory mechanism of GMQ and previously characterized peptide toxins that target the acidic pockets, highlighting that the mechanisms of gating associated with the nonproton binding site (targeted by GMQ) and the acidic pockets (targeted by the peptide toxins) could at least partially overlap during pH-dependent inactivation.

5.1 Rational for using the half-maximal pH of activation and inactivation in our analysis.

Our approach is partially based on the variations of $pH_{0.5}$ of activation, but activation of ASIC channels can be influenced by their inactivation rate, leading in some case to an underestimation of the pH sensitivity for activation (Grunder and Pusch, 2015). The influence of the inactivation rate on activation is not expected to significantly interfere with the interpretation of our data. First, the rate of inactivation principally depends upon the nature of the extracellular domain (Salinas et al., 2009), with similar rates between ASIC1a and ASIC3ECD1a, and between ASIC3 and ASIC1aECD3 (Table 2). Consequently, in the analysis of the contribution of the different domains from ASIC1a and ASIC3 to the pH sensitivity, the influence of the inactivation rate on activation was similar and was therefore canceled by their subtraction in the calculation of the $\Delta pH_{0.5}$ of activation. On the other hand, when constructions with two different extracellular domains were compared, the faster rate of inactivation produced by ECD3 compared to ECD1a probably led to an underestimation of the $pH_{0.5}$ of activation, which is different between both types of constructions. The variation of $pH_{0.5}$ (i.e., $\Delta pH_{0.5}$) between ASIC1a and ASIC1aECD3 or between ASIC3ECD1a and ASIC3 could be similarly overestimated, but the amplitude of this influence, which has been estimated in the model presented by Gründer and Pusch (Grunder and Pusch, 2015) to be of maximum of 0.17 pH unit, remains much smaller than the calculated $\Delta pH_{0.5}$ of activation in our experiments. The pharmacological modulators used, i.e., GMQ, amiloride, mambalgin-1 and PcTx1 have no

significant influence on the different inactivation rates in our protocols (Table 2), and the influence of the inactivation rate on activation was therefore cancelled by the subtraction of the different $pH_{0.5}$ in $\Delta pH_{0.5}$. Finally, possible influence of the inactivation rate on activation was minimized in our cycle analysis approach, where errors on the estimation of the $pH_{0.5}$ of activation canceled each other in the calculation of Zeta, the new variable used in simple cycle analysis in our experiments. The $pH_{0.5}$ measured in our experiments were also not expected to be significantly impacted by the small change in selectivity reported in the original paper on GMQ and measured at pH7.4 (Yu et al., 2010).

5.2 Comparison of the amiloride- and GMQ-dependent effects on ASIC1a and ASIC3, and elements on the amiloride-binding site.

Amiloride and GMQ act both as blockers of ASIC channels through binding into the pore with different efficiency (Alijevic and Kellenberger, 2012). However, GMQ is primarily known as a positive modulator of ASIC3 (Yu et al., 2010) that also modulates ASIC1a (Alijevic and Kellenberger, 2012), and amiloride has a stimulatory effect on ASIC3 (Adams et al., 1999; Li et al., 2011; Waldmann et al., 1997a; Yagi et al., 2006). The effects of GMQ, but not amiloride, on the pH-dependent activation and inactivation of ASIC1a and ASIC3 have been characterized (Alijevic and Kellenberger, 2012). We determined here the effects of amiloride, showing in a back-to-back comparison that they are almost similar to the ones of GMQ. These effects depend on the nature of the extracellular domain (i.e., it is different when acting on ECD1a or ECD3), and their amplitude is modulated by the N/TM/C domains, especially in ASIC3. GMQ and amiloride share a similar mechanism of regulation of the pH-dependent activation, while they show difference in the amplitudes of their effect on the pH-dependent inactivation, which may reflect difference between the molecular structures of these two compounds.

The nature of the binding sites responsible for the stimulatory effects of amiloride on the pH-dependent gating of ASIC3 was not clear, while strong evidence exists for GMQ to act through a nonproton ligand sensing domain (Yu et al., 2010). In a first hypothesis, amiloride has been proposed to bind to the same site based on the observation that the nonproton ligand sensing domain identified for GMQ (Yu et al., 2010) is also required for the paradoxical stimulatory effect of amiloride (Li et al., 2011). Only one nonproton ligand binding site was described per functional trimeric channel (Yu et al., 2010; Yu et al., 2011), which means that independent and purely additive effects of amiloride and GMQ would be expected in this case. The second hypothesis emerged from crystallographic data (Baconguis et al., 2014) and molecular docking (Qadri et al., 2010), which suggest binding of amiloride into the acidic pockets (three per functional channel) but not into the unique nonproton ligand binding site. In this case, a strong cooperativity is expected, as described for protons binding into the different pH-sensors (Zhang et al., 2006), including the three acidic pockets (Vullo et al., 2017). In addition, it has also been shown that the acidic pockets and the nonproton ligand binding site trigger mechanisms that interfere to regulate the gating with a central role of the Palm domain (Vullo et al., 2017), indicating that the mechanisms triggered by these two different sites are indeed not independent.

The question of whether amiloride and GMQ have a common binding site (i.e., the nonproton ligand sensing domain) or not is indirectly addressed by our data. We show first that the gating regulation of ASIC1a and ASIC3 by amiloride and GMQ is for the most part similar, which is consistent with a common binding site for both compounds. We also showed that GMQ alone, or amiloride and GMQ together, act by a purely additive and non-cooperative mechanism on ASIC1a and ASIC3. This excludes binding of these molecules to the three interdependent acidic pockets, or to two different sites, i.e., the acidic pocket and the nonproton ligand binding site, which are not independent of each other (Vullo et al., 2017). Our data are

therefore consistent with the first initial hypothesis proposing a common unique binding site per trimeric channel for amiloride and GMQ.

5.3 Relationship between the window current and the regulation by guanidine compounds.

The window current can be strongly potentiated by amiloride and GMQ in ASIC3 while it failed to induce any in ASIC1a, raising the question of the relationship between these pharmacological agents and the regulation of this physiologically relevant current. The sustained window current in ASIC3 has been associated with the (N/TM/C) domains, which generate a greater closed state instability compared with ASIC1a (Salinas et al., 2009). It was therefore interesting to test if the difference of regulation of ASIC1a and ASIC3 by GMQ (i.e., mainly the potentiating effect of GMQ on the ASIC3 window current) could be supported by the (N/TM/C) domains rather than by the ECD. This is clearly not the case since our data show that the ECD determines the effects of GMQ and amiloride on ASIC1a and ASIC3 (which are however modulated, in their amplitudes, by the (N/TM/C) domains), and that there is no direct link between the potentiating effect of GMQ and the presence or the absence of a window current (as illustrated by chimera ASIC3ECD1a and by ASIC1a, respectively). Amiloride and GMQ induced a broad overlap of the pH-dependent curves of activation and inactivation in ASIC3 because of the combination of both the mechanism of regulation mediated by the extracellular domain (i.e., an alkaline and acidic shift of the pH-dependent activation and inactivation, respectively) and the stronger closed state instability induced by the transmembrane/cytosolic domains (Salinas et al., 2009). Inversely, the amiloride- and GMQ-dependent mechanism of regulation mediated by the extracellular domain of ASIC1a (i.e., an acidic shift of both the pH-dependent activation and inactivation) together with the greater stability of the closed state induced by the transmembrane/cytosolic domains of ASIC1a

compared to the ones of ASIC3 (Salinas et al., 2009), explain why these two compounds failed to generate a window current in ASIC1a.

5.4 GMQ and peptides toxins help to understand how the nonproton ligand-sensor and the acidic pocket dependent-mechanisms interfere during the pH-dependent gating of ASIC1a.

Overlaps between activation and inactivation mechanisms make analysis of the pH-dependent gating of ASIC channels difficult. Activation and inactivation of ASICs involve the extracellular domain and are propagated to the transmembrane domains. These mechanisms are not only functionally coupled but also depend mostly on the same residues (Bonifacio et al., 2014; Liechti et al., 2010). We took advantage of the fact that amiloride and GMQ on one side, and the peptide toxins PcTx1 and mambalgin-1 on the other side, target two different regions in the extracellular domain, a nonproton ligand-sensor (Yu et al., 2010) and the acidic pocket or pH-sensor (Baconguis and Gouaux, 2012; Salinas et al., 2014; Salinas et al., 2006; Schroeder et al., 2014), respectively (Fig. 5G,H), to modulate the pH-dependent gating of ASIC1a. Inversely, protons target almost all domains at the same time. Our data show that the GMQ-dependent mechanism is independent of the mambalgin-1- or PcTx1-dependent mechanisms acting on activation, while regulation of inactivation by GMQ and PcTx1, but not mambalgin-1, overlap. We have combined these data with data of the literature on the conformational changes during the gating of ASICs (Baconguis and Gouaux, 2012; Kellenberger and Schild, 2015; Yang et al., 2009) to build a mechanistic interpretation of our results (Fig. 5G,H). PcTx1 (Fig. 5G) and mambalgin-1 (Fig. 5H) act on activation in a similar way primarily through the Thumb domain connected to the Palm domain (Salinas et al., 2014) (label 3 in Fig. 5G,H). PcTx1 regulates inactivation through the upper Palm and β-Ball domains (Salinas et al., 2014) (labels 1 and 2 in Fig. 5G), whereas GMQ modulates inactivation through the lower Palm domain (Alijevic and Kellenberger, 2012; Yu et al., 2010; Yu et al., 2011) (label 1 in Fig. 5G).

This suggests that the overlap between the mechanisms of regulation by PcTx1 and GMQ during the pH dependent inactivation probably involves the Palm domain (label 1 in Fig. 5G). Mambalgin-1 also interacts with the Palm domain to prevent opening of ASIC1a (Salinas et al., 2014) (label 1' in Fig. 5H), but independently of the effect of GMQ (label 1 in Fig. 5H). More generally, the acidic pockets targeted by the peptide toxins, and the nonproton binding-site targeted by GMQ could be associated with different mechanisms of gating that at least partially overlap during pH-dependent inactivation of ASIC1a.

Acknowledgments

We thank D. Servent, S. Diochot, A. Baron, E. Deval, J. Noël, A. Negm, S. Marra, C. Verkest and M. Chafai for discussions and comments, M. Lazdunski for his support, V. Friend for expert technical assistance, and V. Berthieux for secretarial assistance.

Funding: This work was supported by CNRS, INSERM and the Agence Nationale de la Recherche [grant number ANR-13-BSV4-0009].

Conflict of interest: None.

Author contributions

TB, Acquisition of data, Analysis and interpretation of data, Drafting or revising the article.

EL, Conception and design, Drafting or revising the article.

MS, Conception and design, Acquisition of data, Analysis and interpretation of data, Drafting or revising the article.

Appendix A: Supplementary data

The following is supplementary data related to this article:

Supplemental Figure legends

Supplemental Figure 1. **ASIC3 wild-type and L529A point mutant (ASIC3$^{L/A}$) have the same functional properties. A)** The different sub-domains in ASIC are schematically represented as described by Jasti et al. (Jasti et al., 2007), and only 2 subunits of the trimeric channel are shown for simplicity. Note that the ECD as defined here includes the very upper part of the transmembrane domains (TMs), i.e., the Wrist domain connecting the Thumb and the Palm domains with the TMs, to preserve proper coupling between the extracellular domain and the rest of the channel during pH-dependent gating. **B)** Statistical analysis of the peak current amplitudes associated with the ASIC3 and ASIC3$^{L/A}$ channels and induced by a drop in pH from 7.4 to 5.0 (top), and of the sustained window current at pH7.0 normalized to the peak current (bottom) (n=8-13; *** P<0.001, unpaired t-test). L529A corresponds to a mutation in a consensus motif for internalization closed to the end of the cytoplasmic carboxy-terminus (R…LV) that increased the peak current of ASIC3 by about 3-fold ($I_{peak\text{-}pH5.0}$= 1.14±0.20 and 3.62±0.47 µA for ASIC3 and ASIC3$^{L/A}$, respectively) without affecting the window current ($I_{sustained\text{-}pH7.0}/I_{peak\text{-}pH5.0}$= 1.09±0.20 % and 1.30±0.11 % for ASIC3 and ASIC3$^{L/A}$; P>0.05, unpaired t-test) and the others properties. **C)** Typical current traces showing the same characteristic biphasic current in ASIC3 and ASIC3$^{L/A}$. **D)** The pH-dependent curves of activation (triangle) and inactivation (square) for ASIC3 (black lines; n=5) and ASIC3$^{L/A}$ (red lines; n=6-8) are identical. Solid lines are fits of the mean values of each data point to a sigmoidal dose-response curve with variable slope. The pHs for half-maximal activation and inactivation are not significantly different between ASIC3 and ASIC3$^{L/A}$ (see values in Table 1). **E)** Amiloride inhibited in a similar way the ASIC3 and ASIC3$^{L/A}$ peak currents at pH5.0. Current amplitudes, normalized to amplitude in the absence of amiloride, are plotted as the inverse of a logarithmic function of amiloride concentration. The pIC_{50} values for ASIC3 and ASIC3$^{L/A}$ determined from the fit are $pIC_{50pH5.0+AMI}$=4.14±0.12 (n=6) and 4.16±0.06 (n=7),

P>0.05*;* respectively. **F)** Amiloride similarly activated the ASIC3 and ASIC3$^{L/A}$ currents when applied at pH 7.0 ($pEC_{50pH7.0+AMI}$=3.37±0.02 (n=5) and 3.34±0.03 (n=5), P>0.05*;* respectively. **G)** Activation of the pH7.0-evoked ASIC3 and ASIC3$^{L/A}$ currents by GMQ are also not significantly different ($pEC_{50pH7.0+GMQ}$=2.99±0.02 (n=9) and 2.94±0.06 (n=8), P>0.05*;* respectively).

Supplemental Figure 2. **Sequence alignement of rat ASIC1a and ASIC3.** TM1 and TM2 indicate the position of transmembane domains 1 and 2. The cytosolic amino- and carboxy-terminal domains are noted N and C domains, respectively. The extracellular domain including the Wrist domain is shown in red and noted ECD. Tyr 71 and Trp 287 composing the contact between the Thumb domain and the TM1 domain are marked by green circles.

References

Adams, C. M., Snyder, P. M., Welsh, M. J., 1999. Paradoxical stimulation of a DEG/ENaC channel by amiloride. J Biol Chem 274, 15500-15504.

Alijevic, O., Kellenberger, S., 2012. Subtype-specific modulation of acid-sensing ion channel (ASIC) function by 2-guanidine-4-methylquinazoline. J Biol Chem 287, 36059-36070. doi: 10.1074/jbc.M112.360487.

Baconguis, I., Bohlen, C. J., Goehring, A., Julius, D., Gouaux, E., 2014. X-ray structure of acid-sensing ion channel 1-snake toxin complex reveals open state of a Na(+)-selective channel. Cell 156, 717-729. doi: 10.1016/j.cell.2014.01.011.

Baconguis, I., Gouaux, E., 2012. Structural plasticity and dynamic selectivity of acid-sensing ion channel-spider toxin complexes. Nature 489, 400-405. doi: 10.1038/nature11375.

Bonifacio, G., Lelli, C. I., Kellenberger, S., 2014. Protonation controls ASIC1a activity via coordinated movements in multiple domains. J Gen Physiol 143, 105-118. doi: 10.1085/jgp.201311053.

Chen, X., Kalbacher, H., Grunder, S., 2005. The tarantula toxin psalmotoxin 1 inhibits acid-sensing ion channel (ASIC) 1a by increasing its apparent H+ affinity. J Gen Physiol 126, 71-79. doi: 10.1085/jgp.200509303.

Chen, X., Kalbacher, H., Grunder, S., 2006. Interaction of Acid-sensing Ion Channel (ASIC) 1 with the Tarantula Toxin Psalmotoxin 1 is State Dependent. J Gen Physiol 127, 267-276. doi: 10.1085/jgp.200509409.

Della Vecchia, M. C., Rued, A. C., Carattino, M. D., 2013. Gating transitions in the palm domain of ASIC1a. J Biol Chem 288, 5487-5495. doi: 10.1074/jbc.M112.441964.

Deval, E., Lingueglia, E., 2008. Les canaux ioniques ASIC : des senseurs de l'acidification extracellulaire dans le système nerveux. Biofutur 294, 49-51.

Diochot, S., Baron, A., Salinas, M., Douguet, D., Scarzello, S., Dabert-Gay, A. S., Debayle, D., Friend, V., Alloui, A., Lazdunski, M., Lingueglia, E., 2012. Black mamba venom peptides target acid-sensing ion channels to abolish pain. Nature 490, 552-555. doi: 10.1038/nature11494.

Friese, M. A., Craner, M. J., Etzensperger, R., Vergo, S., Wemmie, J. A., Welsh, M. J., Vincent, A., Fugger, L., 2007. Acid-sensing ion channel-1 contributes to axonal degeneration in autoimmune inflammation of the central nervous system. Nat Med 13, 1483-1489.

Gonzales, E. B., Kawate, T., Gouaux, E., 2009. Pore architecture and ion sites in acid-sensing ion channels and P2X receptors. Nature 460, 599-604. doi: 10.1038/nature08218.

Grunder, S., Pusch, M., 2015. Biophysical properties of acid-sensing ion channels (ASICs). Neuropharmacology 94, 9-18. doi: 10.1016/j.neuropharm.2014.12.016.

Hidalgo, P., MacKinnon, R., 1995. Revealing the architecture of a K+ channel pore through mutant cycles with a peptide inhibitor. Science 268, 307-310.

Jasti, J., Furukawa, H., Gonzales, E. B., Gouaux, E., 2007. Structure of acid-sensing ion channel 1 at 1.9 A resolution and low pH. Nature 449, 316-323. doi: 10.1038/nature06163.

Kellenberger, S., Schild, L., 2015. International Union of Basic and Clinical Pharmacology. XCI. structure, function, and pharmacology of acid-sensing ion channels and the epithelial Na+ channel. Pharmacol Rev 67, 1-35. doi: 10.1124/pr.114.009225.

Krauson, A. J., Rued, A. C., Carattino, M. D., 2013. Independent contribution of extracellular proton binding sites to ASIC1a activation. J Biol Chem 288, 34375-34383. doi: 10.1074/jbc.M113.504324.

Li, T., Yang, Y., Canessa, C. M., 2009. Interaction of the aromatics Tyr-72/Trp-288 in the interface of the extracellular and transmembrane domains is essential for proton gating of acid-sensing ion channels. J Biol Chem 284, 4689-4694. doi: 10.1074/jbc.M805302200.

Li, W. G., Yu, Y., Huang, C., Cao, H., Xu, T. L., 2011. Nonproton ligand sensing domain is required for paradoxical stimulation of acid-sensing ion channel 3 (ASIC3) channels by amiloride. J Biol Chem 286, 42635-42646. doi: 10.1074/jbc.M111.289058.

Liechti, L. A., Berneche, S., Bargeton, B., Iwaszkiewicz, J., Roy, S., Michielin, O., Kellenberger, S., 2010. A combined computational and functional approach identifies new residues involved in pH-dependent gating of ASIC1a. J Biol Chem 285, 16315-16329. doi: 10.1074/jbc.M109.092015.

Marra, S., Ferru-Clement, R., Breuil, V., Delaunay, A., Christin, M., Friend, V., Sebille, S., Cognard, C., Ferreira, T., Roux, C., Euller-Ziegler, L., Noel, J., Lingueglia, E., Deval, E., 2016. Non-acidic

activation of pain-related Acid-Sensing Ion Channel 3 by lipids. EMBO J 35, 414-428. doi: 10.15252/embj.201592335.

Mazzuca, M., Heurteaux, C., Alloui, A., Diochot, S., Baron, A., Voilley, N., Blondeau, N., Escoubas, P., Gelot, A., Cupo, A., Zimmer, A., Zimmer, A. M., Eschalier, A., Lazdunski, M., 2007. A tarantula peptide against pain via ASIC1a channels and opioid mechanisms. Nat Neurosci 10, 943-945. doi: 10.1038/nn1940.

Meng, Q. Y., Wang, W., Chen, X. N., Xu, T. L., Zhou, J. N., 2009. Distribution of acid-sensing ion channel 3 in the rat hypothalamus. Neuroscience 159, 1126-1134. doi: 10.1016/j.neuroscience.2009.01.069.

Mildvan, A. S., Weber, D. J., Kuliopulos, A., 1992. Quantitative interpretations of double mutations of enzymes. Arch Biochem Biophys 294, 327-340.

Mourier, G., Salinas, M., Kessler, P., Stura, E. A., Leblanc, M., Tepshi, L., Besson, T., Diochot, S., Baron, A., Douguet, D., Lingueglia, E., Servent, D., 2016. Mambalgin-1 Pain-relieving Peptide, Stepwise Solid-phase Synthesis, Crystal Structure, and Functional Domain for Acid-sensing Ion Channel 1a Inhibition. J Biol Chem 291, 2616-2629. doi: 10.1074/jbc.M115.702373.

Noel, J., Salinas, M., Baron, A., Diochot, S., Deval, E., Lingueglia, E., 2010. Current perspectives on acid-sensing ion channels: new advances and therapeutic implications. Expert Rev Clin Pharmacol 3, 331-346. doi: 10.1586/ecp.10.13.

Paukert, M., Chen, X., Polleichtner, G., Schindelin, H., Grunder, S., 2008. Candidate amino acids involved in H+ gating of acid-sensing ion channel 1a. J Biol Chem 283, 572-581. doi: 10.1074/jbc.M706811200.

Qadri, Y. J., Song, Y., Fuller, C. M., Benos, D. J., 2010. Amiloride docking to acid-sensing ion channel-1. J Biol Chem 285, 9627-9635. doi: 10.1074/jbc.M109.082735.

Salinas, M., Besson, T., Delettre, Q., Diochot, S., Boulakirba, S., Douguet, D., Lingueglia, E., 2014. Binding site and inhibitory mechanism of the mambalgin-2 pain-relieving peptide on acid-sensing ion channel 1a. J Biol Chem 289, 13363-13373. doi: 10.1074/jbc.M114.561076.

Salinas, M., Lazdunski, M., Lingueglia, E., 2009. Structural elements for the generation of sustained currents by the acid pain sensor ASIC3. J Biol Chem 284, 31851-31859. doi: 10.1074/jbc.M109.043984.

Salinas, M., Rash, L. D., Baron, A., Lambeau, G., Escoubas, P., Lazdunski, M., 2006. The receptor site of the spider toxin PcTx1 on the proton-gated cation channel ASIC1a. J Physiol 570, 339-354. doi: 10.1113/jphysiol.2005.095810.

Schroeder, C. I., Rash, L. D., Vila-Farres, X., Rosengren, K. J., Mobli, M., King, G. F., Alewood, P. F., Craik, D. J., Durek, T., 2014. Chemical synthesis, 3D structure, and ASIC binding site of the toxin mambalgin-2. Angew Chem Int Ed Engl 53, 1017-1020. doi: 10.1002/anie.201308898.

Schuhmacher, L. N., Smith, E. S., 2016. Expression of acid-sensing ion channels and selection of reference genes in mouse and naked mole rat. Mol Brain 9, 97. doi: 10.1186/s13041-016-0279-2.

Schuhmacher, L. N., Srivats, S., Smith, E. S., 2015. Structural domains underlying the activation of acid-sensing ion channel 2a. Mol Pharmacol 87, 561-571. doi: 10.1124/mol.114.096909.

Vullo, S., Bonifacio, G., Roy, S., Johner, N., Berneche, S., Kellenberger, S., 2017. Conformational dynamics and role of the acidic pocket in ASIC pH-dependent gating. Proc Natl Acad Sci U S A. doi: 10.1073/pnas.1620560114.

Waldmann, R., Bassilana, F., de Weille, J., Champigny, G., Heurteaux, C., Lazdunski, M., 1997a. Molecular cloning of a non-inactivating proton-gated Na+ channel specific for sensory neurons. J Biol Chem 272, 20975-20978.

Waldmann, R., Champigny, G., Bassilana, F., Heurteaux, C., Lazdunski, M., 1997b. A proton-gated cation channel involved in acid-sensing. Nature 386, 173-177. doi: 10.1038/386173a0.

Wemmie, J. A., Askwith, C. C., Lamani, E., Cassell, M. D., Freeman, J. H., Jr., Welsh, M. J., 2003. Acid-sensing ion channel 1 is localized in brain regions with high synaptic density and contributes to fear conditioning. J Neurosci 23, 5496-5502.

Wemmie, J. A., Taugher, R. J., Kreple, C. J., 2013. Acid-sensing ion channels in pain and disease. Nat Rev Neurosci 14, 461-471. doi: 10.1038/nrn3529.

Xiong, Z. G., Zhu, X. M., Chu, X. P., Minami, M., Hey, J., Wei, W. L., MacDonald, J. F., Wemmie, J. A., Price, M. P., Welsh, M. J., Simon, R. P., 2004. Neuroprotection in ischemia: blocking calcium-permeable acid-sensing ion channels. Cell 118, 687-698. doi: 10.1016/j.cell.2004.08.026.

Yagi, J., Wenk, H. N., Naves, L. A., McCleskey, E. W., 2006. Sustained currents through ASIC3 ion channels at the modest pH changes that occur during myocardial ischemia. Circ Res 99, 501-509. doi: 10.1161/01.RES.0000238388.79295.4c.

Yang, H., Yu, Y., Li, W. G., Yu, F., Cao, H., Xu, T. L., Jiang, H., 2009. Inherent dynamics of the acid-sensing ion channel 1 correlates with the gating mechanism. PLoS Biol 7, e1000151. doi: 10.1371/journal.pbio.1000151.

Yu, Y., Chen, Z., Li, W. G., Cao, H., Feng, E. G., Yu, F., Liu, H., Jiang, H., Xu, T. L., 2010. A nonproton ligand sensor in the acid-sensing ion channel. Neuron 68, 61-72. doi: 10.1016/j.neuron.2010.09.001.

Yu, Y., Li, W. G., Chen, Z., Cao, H., Yang, H., Jiang, H., Xu, T. L., 2011. Atomic level characterization of the nonproton ligand-sensing domain of ASIC3 channels. J Biol Chem 286, 24996-25006. doi: 10.1074/jbc.M111.239558.

Zhang, P., Sigworth, F. J., Canessa, C. M., 2006. Gating of Acid-sensitive Ion Channel-1: Release of Ca^{2+} Block vs. Allosteric Mechanism. J Gen Physiol 127, 109-117.

	$pH_{0.5}$inact	$pH_{0.5}$act	$\Delta pH_{0.5}$inact from control	$\Delta pH_{0.5}$act from control
ASIC3	7.17±0.01^{ns}	6.19±0.04^{ns}	-	-
ASIC3$^{L/A}$	**7.16±0.01**	**6.17±0.02**	-	-
ASIC3$^{L/A}$+GMQ (1mM)	6.44±0.02***	7.12±0.04***	**-0.72±0.03*****	**+0.95±0.06*****
ASIC3$^{L/A}$+AMI (1mM)	6.92±0.01***	7.06±0.04***	-0.24±0.02$^{***\delta\delta\delta}$	+0.89±0.06^{***ns}
ASIC1a	**7.16±0.01**	**6.39±0.02**	-	-
ASIC1a+GMQ (1mM)	6.99±0.01***	6.07±0.02**	**-0.17±0.02*****	**-0.32±0.04****
ASIC1a+AMI (1mM)	7.13±0.01^{ns}	6.25±0.04*	-0.03±0.02$^{ns\delta\delta\delta}$	-0.14±0.06^{*ns}
ASIC3ECD1a	**7.23±0.01**	**6.93±0.03**	-	-
ASIC3ECD1a+GMQ (1mM)	7.12±0.01***	6.62±0.03*	**-0.11±0.02*****	**-0.31±0.06***
ASIC3ECD1a+AMI (1mM)	7.09±0.01**	6.58±0.04*	-0.14±0.02^{**ns}	-0.35±0.07^{*ns}
ASIC1aECD3	**7.08±0.01**	**5.64±0.03**	-	-
ASIC1aECD3+GMQ (1mM)	6.80±0.02***	5.78±0.03*	**-0.28±0.03*****	**+0.14±0.06***
ASIC1aECD3+AMI (1mM)	6.94±0.01***	5.89±0.02**	-0.14±0.02$^{***\delta\delta}$	+0.25±0.05^{**ns}
ASIC1a+AMI (1mM)	***7.13±0.01***	***6.25±0.04***	-	-
ASIC1a+GMQ (1mM)/AMI (1mM)	6.94±0.02***	6.03±0.03*	-0.19±0.03***	-0.22±0.07*
ASIC3$^{L/A}$+AMI (1mM)	***6.92±0.01***	***7.06±0.04***	-	-
ASIC3$^{L/A}$+GMQ (1mM)/AMI (1mM)	6.19±0.03***	7.24±0.03**	-0.73±0.04***	+0.18±0.07**
ASIC3$^{L/A}$		***6.17±0.02***		-
ASIC3$^{L/A}$+GMQ (0.5mM)		6.63±0.04***		**+0.46±0.06*****
ASIC3$^{L/A}$+AMI (0.5mM)		6.70±0.04***		**+0.53±0.06*****
ASIC3$^{L/A}$+GMQ(0.5mM)/AMI (0.5mM)		7.13±0.02***		+0.96±0.04$^{***\delta\delta\delta}$
ASIC3$^{L/A}$+GMQ (1mM)		7.12±0.04***		+0.95±0.06$^{***\delta\delta\delta}$
ASIC1a	**7.16±0.01**	**6.39±0.02**	-	-
ASIC1a+PcTx1 (10nM)	7.53±0.01***	6.37±0.02^{ns}	+0.37±0.02***	-0.02±0.04^{ns}
ASIC1a+Mamb1(10nM)	7.12±0.01*	5.70±0.03***	-0.04±0.02*	-0.69±0.05***
ASIC1a+PcTx1 (10nM)	**7.53±0.01**	**6.37±0.02**	-	-
ASIC1a+GMQ(1mM)/PcTx1(10nM)	7.14±0.01***	6.03±0.03***	-0.39±0.02***	-0.34±0.05***
ASIC1a+Mamb1(10nM)	**7.12±0.01**	**5.70±0.03**	-	-
ASIC1a+GMQ(1mM)/Mamb1(10nM)	6.96±0.01***	5.42±0.03**	-0.16±0.02***	-0.28±0.06**

Table 1. $pH_{0.5}$ of activation and inactivation in the absence or in the presence of different pharmacological agents. Half-maximal pH of inactivation ($pH_{0.5}$inact) and activation ($pH_{0.5}$act) of ASIC1a, ASIC3, ASIC3$^{L/A}$, ASIC3ECD1a and ASIC1aECD3 treated or not with GMQ, amiloride (AMI), GMQ/AMI, peptides or GMQ/peptides. Variations of pH sensitivity ($\Delta pH_{0.5}$) induced by the different treatments are calculated as follow: $\Delta pH_{0.5}$=$pH_{0.5}$[GMQ and/or AMI and/or peptides] - $pH_{0.5}$control (noted in bold). A positive or negative value of $\Delta pH_{0.5}$ indicates greater or smaller pH sensitivity, respectively. **$pH_{0.5}$:** Mean ± SEM, one-way analysis of variance followed by Tukey's multiple comparison test: ^{ns} P>0.05, * P<0.05, ** P<0.01, *** P<0.001 compared to control condition (indicated in bold). **$\Delta pH_{0.5}$:** difference of Means ± sum of SEM as indicated in Theory/calculation (paragraph 3.3). Statistical significances of $\Delta pH_{0.5}$ were calculated from the direct comparison of the initial $pH_{0.5}$ (^{ns} P>0.05, * P<0.05, ** P<0.01 *** P<0.001; when compared with control conditions in bold in the first two columns, and ^{ns} P>0.05, $^{\delta}$ P<0.05, $^{\delta\delta}$ P<0.01, $^{\delta\delta\delta}$ P<0.001; when compared with control conditions in bold in the two last columns).

	τinact (s)	n
ASIC3$^{L/A}$	**1.40±0. 08**	**83**
ASIC3$^{L/A}$+GMQ (1mM)	1.51±0.22^{ns}	12
ASIC3$^{L/A}$+AMI (1mM)	1.49±0.16^{ns}	21
ASIC1a	**4.87±0.39**	**57**
ASIC1a+GMQ (1mM)	4.17±0.39 ^{ns}	15
ASIC1a+AMI (1mM)	6.25±0.31 ^{ns}	13
ASIC1a+PcTx1 (10nM) (τ_{inact} at pH5.0)	5.73±0.36 ^{ns}	7
ASIC1a+PcTx1 (10nM) (τ_{inact} at pH6.0/6.5)	6.78±0.68 ^{ns}	10
ASIC1a+Mamb1 (10nM)	4.43±0.29 ^{ns}	17
ASIC1aECD3	**0.70±0.05**	**76**
ASIC1aECD3+GMQ (1mM)	0.68±0.07 ^{ns}	33
ASIC1aECD3+AMI (1mM)	0.72±0.06 ^{ns}	17
ASIC3ECD1a	**8.99±0.35**	**87**
ASIC3ECD1a+GMQ (1mM)	10.41±0.68 ^{ns}	12
ASIC3ECD1a+AMI (1mM)	9.43±0.59 ^{ns}	12

Table 2. Rate of inactivation in the absence or in the presence of different pharmacological agents. Rate of inactivation (τ inact) of ASIC1a, ASIC3$^{L/A}$, ASIC3ECD1a and ASIC1aECD3 treated or not with GMQ, amiloride (AMI), or peptides measured on the current traces used to establish the pH-dependent curves of activation. Amiloride, GMQ and PcTx1 were co-applied with the pH test, and mambalgin-1 was applied at pH8.0 before the pH stimulation in view to test its effect on the closed state of the channel. Note that during the protocol of activation, PcTx1 was co-applied with the pH test to evaluate its effect only on the open state of the cannel, i.e., on the activation mechanism (binding of PcTx1 is state dependent and is able to stabilize both the inactivated and the open states). With this protocol, PcTx1 did not strongly affect the rate of inactivation and therefore prevented possible influence on the determination of the $pH_{0.5}$ of activation. The τ inactivation (τ_{inact}) are calculated with a standard exponential. Mean ± SEM, one-way analysis of variance with Newman-Keuls multiple comparison test: ^{ns} P>0.05 and *** P<0.001 compared to control condition (indicated in bold).

Figures and legends

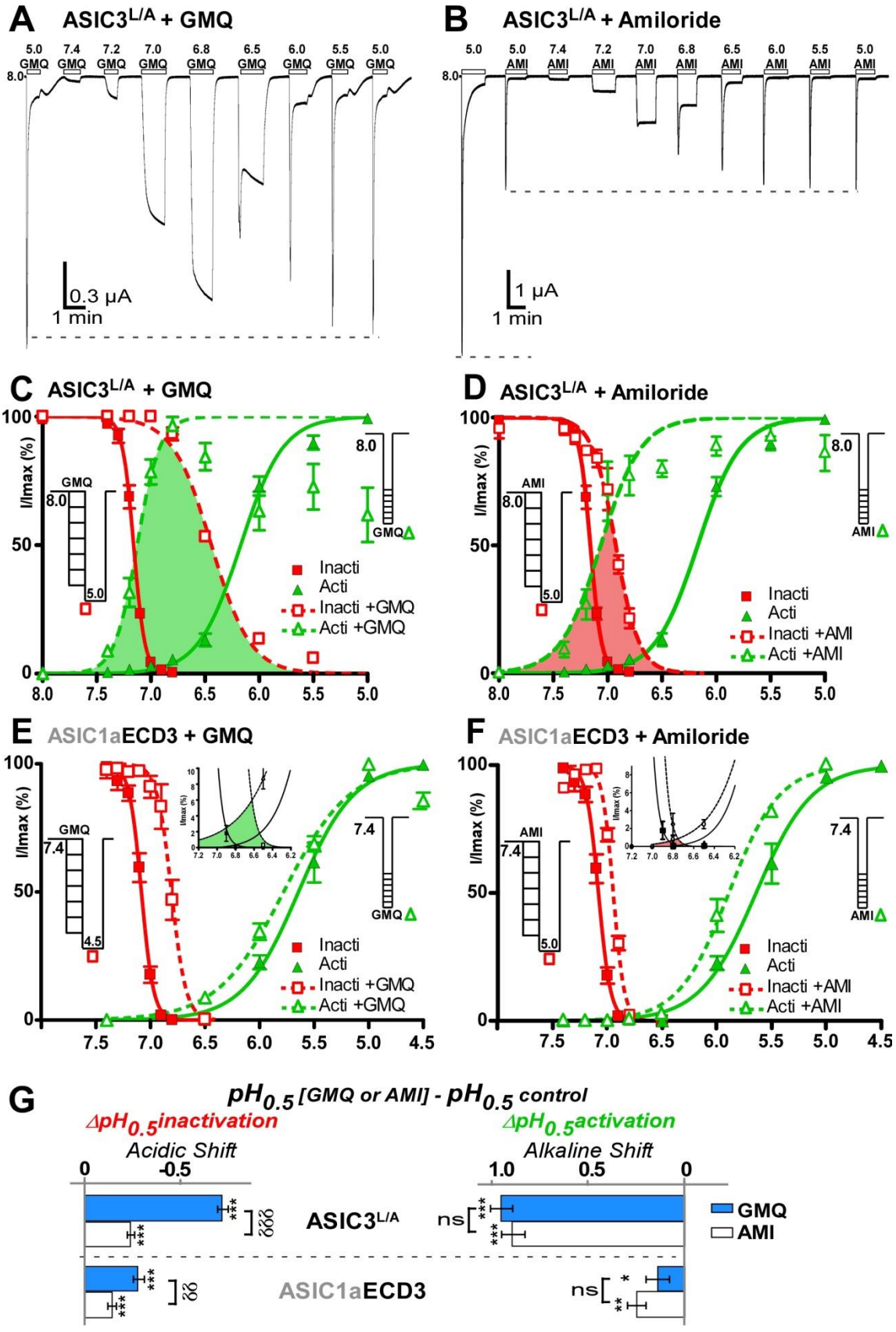

Figure 1. Influence of the ECD3 and of the (N/TM/C) domains on the effect of amiloride and GMQ. A) Typical current trace of ASIC3 $^{L/A}$ generated by application of different pH in the presence of 1 mM GMQ. The currents evoked at different pH from holding pH8.0 are used to trace the activation curve shown in C. **B)** Typical current trace of ASIC3$^{L/A}$ in the presence of 1 mM amiloride using the same protocol as in A. The currents evoked at different pH from holding pH8.0 are used to trace the activation curve shown in D. **C-F)** pH-dependent curves of activation (green; n=6-9) and inactivation (red; n=5-10) for ASIC3 $^{L/A}$ (C,D) and ASIC1aECD3 (E,F) in the absence or in the presence of 1 mM GMQ (C,E) or 1 mM amiloride (D,F). Protocols used for activation and inactivation are shown beside the curves. See Table 1 for the corresponding $pH_{0.5}$ values. In some cases (C,D), activation becomes more pH-sensitive than inactivation, leading to a maximum current value reached at a pH where only the activation process is present, and then to decreased values when inactivation takes place at lower pHs. **G)** Graph showing the variations of $pH_{0.5}$ of activation and inactivation induced by GMQ or amiloride (1 mM) from control conditions. The values of $\Delta pH_{0.5}$ and their statistical analysis are exposed in Table 1.

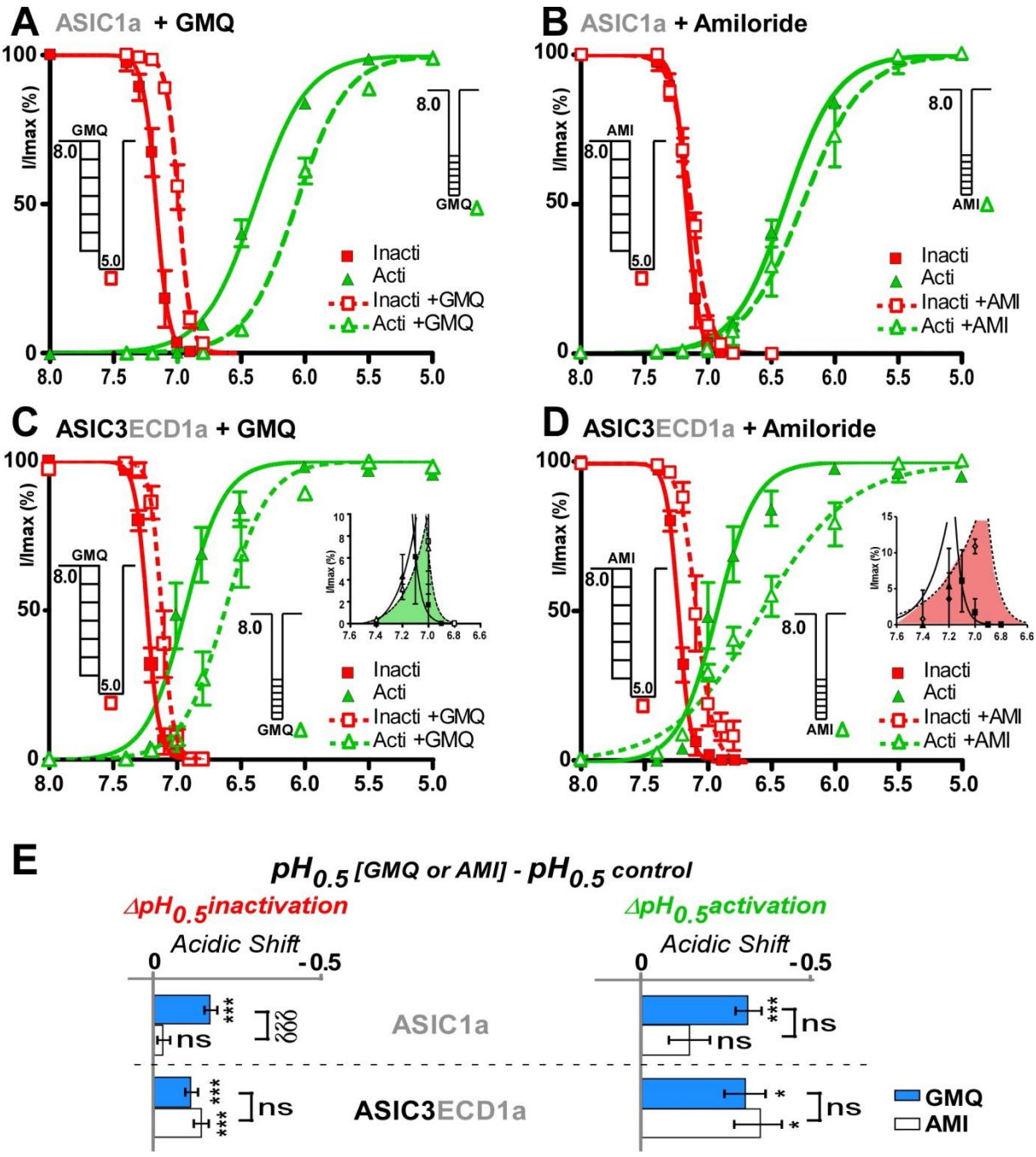

Figure 2. Influence of the ECD1a and of the (N/TM/C) domains on the effect of amiloride and GMQ. A-D) pH-dependent curves of activation (green; n=5-11) and inactivation (red; n=5-8) for ASIC1a (A,B) and ASIC1aECD3 (C,D) in the absence or in the presence of 1 mM GMQ (A,C) or 1 mM amiloride (B,D). Protocols used for activation and inactivation are shown beside the curves. See Table 1 for the corresponding $pH_{0.5}$ values. The overlap of the activation and inactivation curves in C and D are magnified in inset to show the acidic shift of the window current. **E)** Graph showing the variations of $pH_{0.5}$ of activation and inactivation induced by GMQ or amiloride (1 mM) from control. The values of $\Delta pH_{0.5}$ and their statistical analysis are exposed in Table 1**.**

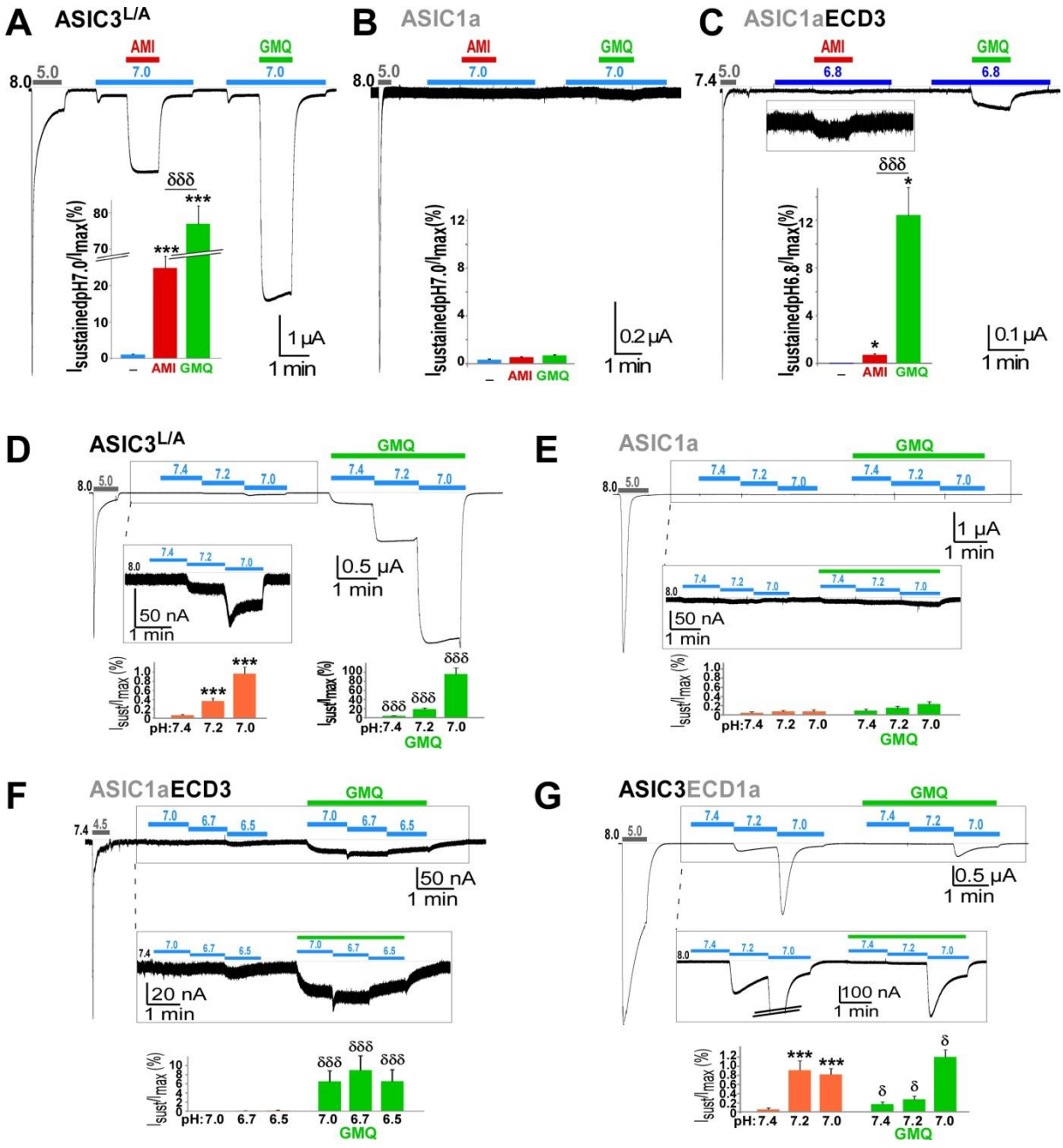

Figure 3. Effect of amiloride and GMQ on the sustained window current at moderate pH. **A-C)** Effects of amiloride and GMQ on the window current generated by moderate acidification (pH 6.8-7.0). Application of 1 mM amiloride or 1 mM GMQ during the pH pulse potentiates or induces a sustained window current. (Inset in A: $I_{sustained\ pH7.0}/I_{peak\text{-}pH5.0}$= 1.1±0.1 %, 25±3 % and 77±5 %, respectively; inset in B: $I_{sustained\ pH7.0}/I_{peak\text{-}pH5.0}$=0.4±0.1 %, 0.6±0.1 % and 0.8±0.1 %, respectively; inset in C: $I_{sustained\ pH6.8}/I_{peak\text{-}pH5.0}$=0.01±0.01 %, 0.7±0.1 % and 12.5±2.3 % for moderate pH alone, amiloride and GMQ, respectively). **D-G)** Measure of the sustained window current in $ASIC3^{L/A}$ (D), ASIC1a (E), ASIC1aECD3 (F) and ASIC3ECD1a (G) with 3 successive pH steps with or without 1 mM GMQ, and statistical difference between both conditions analyzed with nonparametric, paired t-test, Wilcoxon signed rank test (n=6-12): ^{ns} P>0.05, $^{\delta}$ P < 0.05; $^{\delta\delta}$ P < 0.01; $^{\delta\delta\delta}$ P < 0.001. For the conditions without GMQ treatment, the statistical differences with the control pH 7.4 are noted *** P<0.001. The current was magnified when necessary (inset).

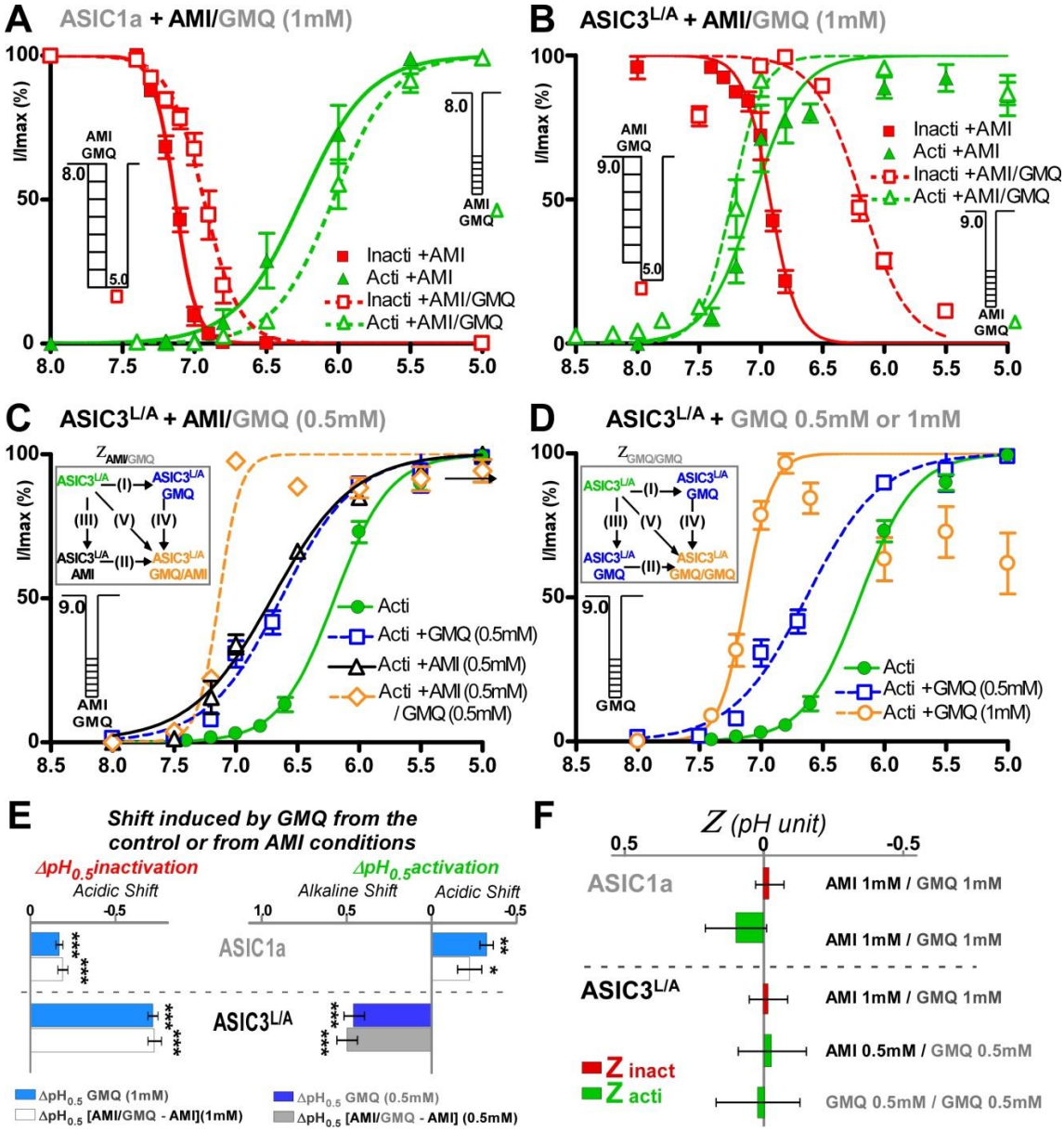

Figure 4. Amiloride and GMQ have no cooperative effect. A-B) pH-dependent curves of activation (green; n=6-9) and inactivation (red; n=5) for ASIC1a and ASIC3$^{L/A}$ in the presence of 1 mM amiloride plus 1 mM GMQ compared to control condition with amiloride alone. The corresponding $pH_{0.5}$ values are shown in Table 1. Protocols are displayed beside the curves. **C-D)** pH-dependent curves of activation for ASIC3$^{L/A}$ in the absence (green in C and D), and in the presence of 0.5 mM or 1 mM GMQ, of 0.5 mM amiloride, or of 0.5 mM amiloride plus 0.5 mM GMQ (n=5). Protocols used are indicated beside the curves. Insets, cycle analysis graph. The corresponding $pH_{0.5}$ values and their variations are listed in Table 1. In some cases, activation becomes more pH-sensitive than inactivation, leading to a maximum current value reached at ~pH7.0 (i.e., when only the activation process is present), and then to decreased values at pHs lower than 7.0 when inactivation takes place (see for example current trace in Fig. 1A). **E)** Histograms reporting the shifts of $pH_{0.5}$ induced by GMQ alone (from Figs. 1 and 2) or by GMQ in the presence of amiloride (calculated from the curves shown in A-D). The values of $\Delta pH_{0.5}$ and their statistical analysis are exposed in Table 1. **F**) Calculated Zeta values for activation (green) and inactivation (red) for the different conditions shown in A-D (deduced from the cycle analysis graphs shown in inset in C and D, see Materials and Methods, paragraph 3.2).

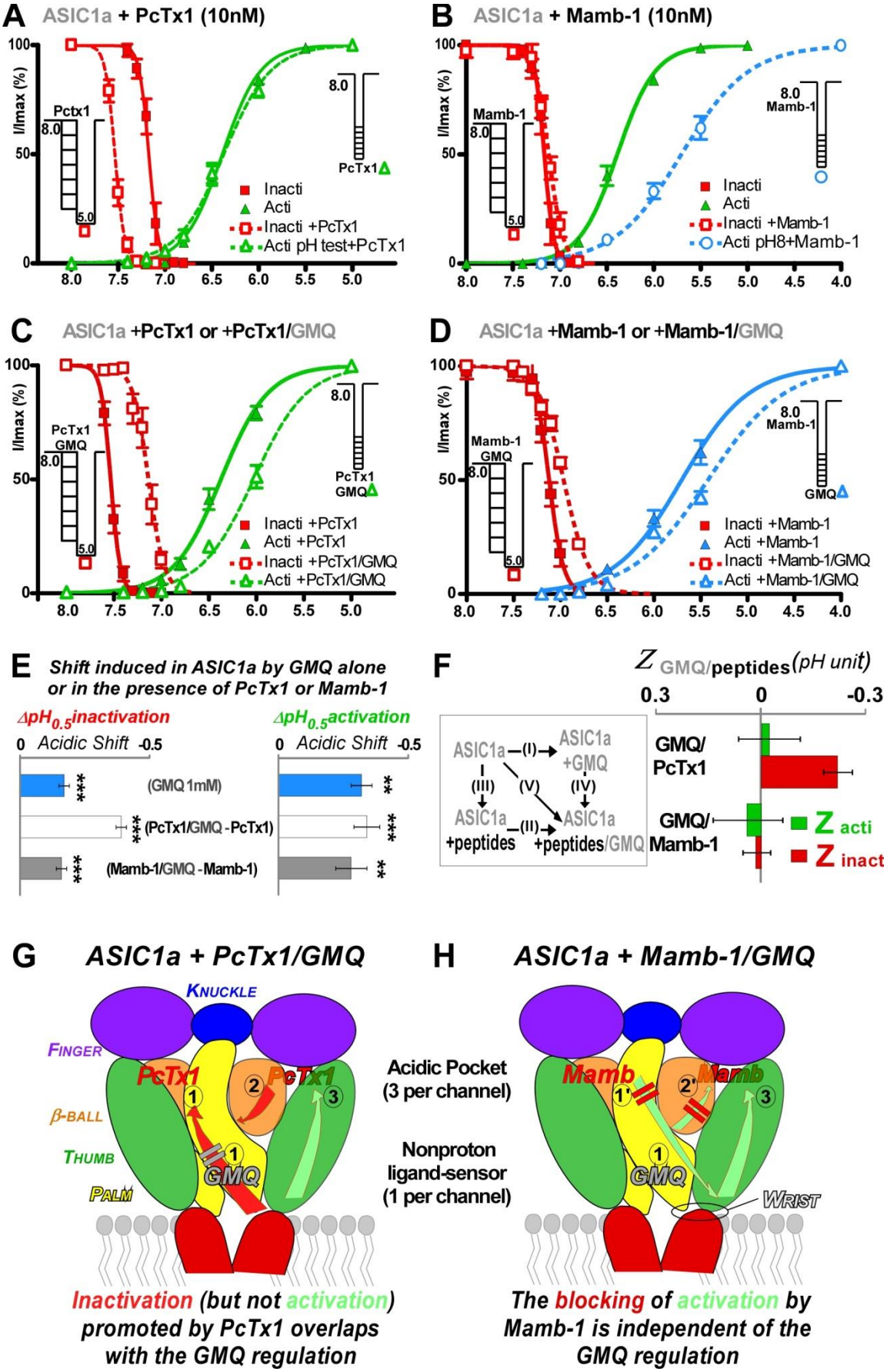
A ASIC1a + PcTx1 (10nM)
I/Imax (%)
PcTx1
8.0
5.0
Inacti
Acti
Inacti +PcTx1
Acti pH test+PcTx1
B ASIC1a + Mamb-1 (10nM)
Mamb-1
Inacti
Acti
Inacti +Mamb-1
Acti pH8+Mamb-1
C ASIC1a +PcTx1 or +PcTx1/GMQ
PcTx1 GMQ
Inacti +PcTx1
Acti +PcTx1
Inacti +PcTx1/GMQ
Acti +PcTx1/GMQ
D ASIC1a +Mamb-1 or +Mamb-1/GMQ
Mamb-1 GMQ
Inacti +Mamb-1
Acti +Mamb-1
Inacti +Mamb-1/GMQ
Acti +Mamb-1/GMQ
E Shift induced in ASIC1a by GMQ alone or in the presence of PcTx1 or Mamb-1
ΔpH0.5 inactivation
ΔpH0.5 activation
Acidic Shift
(GMQ 1mM)
(PcTx1/GMQ - PcTx1)
(Mamb-1/GMQ - Mamb-1)
F
Z GMQ/peptides (pH unit)
ASIC1a
ASIC1a +GMQ
ASIC1a +peptides
ASIC1a +peptides/GMQ
GMQ/ PcTx1
GMQ/ Mamb-1
Z acti
Z inact
G ASIC1a + PcTx1/GMQ
KNUCKLE
FINGER
β-BALL
THUMB
PALM
PcTx1
GMQ
H ASIC1a + Mamb-1/GMQ
Mamb
WRIST
Acidic Pocket (3 per channel)
Nonproton ligand-sensor (1 per channel)
Inactivation (but not activation) promoted by PcTx1 overlaps with the GMQ regulation
The blocking of activation by Mamb-1 is independent of the GMQ regulation

Figure 5. Comparison of the mechanism of action of GMQ and PcTx1 or mambalgin-1 in ASIC1a. A-B) pH-dependent curves of activation (green or blue; n=6-11) and inactivation (red; n=5) in the presence of 10 nM PcTx1 (A) or 10 nM mambalgin-1 (B) compared with control conditions. **C-D)** pH-dependent curves of activation (green or blue; n=6-9) and inactivation (red; n=5-9) of ASIC1a in the presence of 1 mM GMQ plus 10 nM PcTx1 (C) or plus 10 nM mambalgin-1 (D), compared to control conditions with only PcTx1 or mambalgin-1 (same data as in A and B). See Table 1 for the corresponding $pH_{0.5}$ values. Protocols used are shown besides the curves. For activation, PcTx1 was applied during the pH pulses, and mambalgin-1 was applied in the holding pH. **E)** Histograms reporting the shifts of $pH_{0.5}$ induced by GMQ alone or by GMQ in the presence of PcTx1 or mambalgin-1 (calculated from the curves shown in C and D)**.** The values of $\Delta pH_{0.5}$ and their statistical analysis are exposed in Table 1. **F)** Graphical representation of the Zeta values calculated from the cycle analysis graph shown on the left. **G and H**) Graphical representation of the possible overlap (grey bars) of the GMQ regulation through the nonproton ligand binding-site at the lower part of the Palm domain (1) (Alijevic and Kellenberger, 2012; Yu et al., 2010; Yu et al., 2011), with the two different pH-sensor trapping mechanisms described for PcTx1 (G) and mambalgin-1 (H) (Salinas et al., 2014) that involve the acidic pockets. The different sub-domains of ASIC1a are schematically represented as described by Jasti et al. (Jasti et al., 2007)(see also Suppl. Fig. 1A), and only 2 subunits of the trimeric channel are shown for simplicity. Some of the conformational changes associated with activation (green arrows) and inactivation (red arrows) and reported in the literature are represented (only in one subunit for clarity). PcTx1 (G) promotes activation (green arrows) via the Thumb domain (3) and promotes inactivation (red arrows) via the Palm (1) and the β-Ball (2) domains (Salinas et al., 2014). Mambalgin-1 (Mamb-1; H) promotes activation (green arrows) via the Thumb domain (3) similarly to PcTx1 but also blocks activation (green arrows with red bars) via the Palm (1') and/or the β-Ball (2') domains (Salinas et al., 2014).

Supplementary figures: Besson et al.

Pharmacological modulation of Acid-Sensing Ion Channels 1a and 3 by amiloride and 2-guanidine-4-methylquinazoline (GMQ)

Thomas Besson[1,2] , Eric Lingueglia[1,2*#] and Miguel Salinas[1,2*#]

[1]Université Côte d'Azur, CNRS, IPMC, France

[2]LabEx Ion Channel Science and Therapeutics, IPMC, France

 # Equivalent last authors

***Address for correspondence**

Drs Miguel SALINAS and Eric LINGUEGLIA : CNRS, Institut de Pharmacologie Moléculaire et Cellulaire, UMR7275, 06560 Valbonne, France Tel.: 33 4 93 95 34 23; Fax: 33 4 93 95 77 08; E-mail: lingueglia@ipmc.cnrs.fr and salinas@ipmc.cnrs.fr.

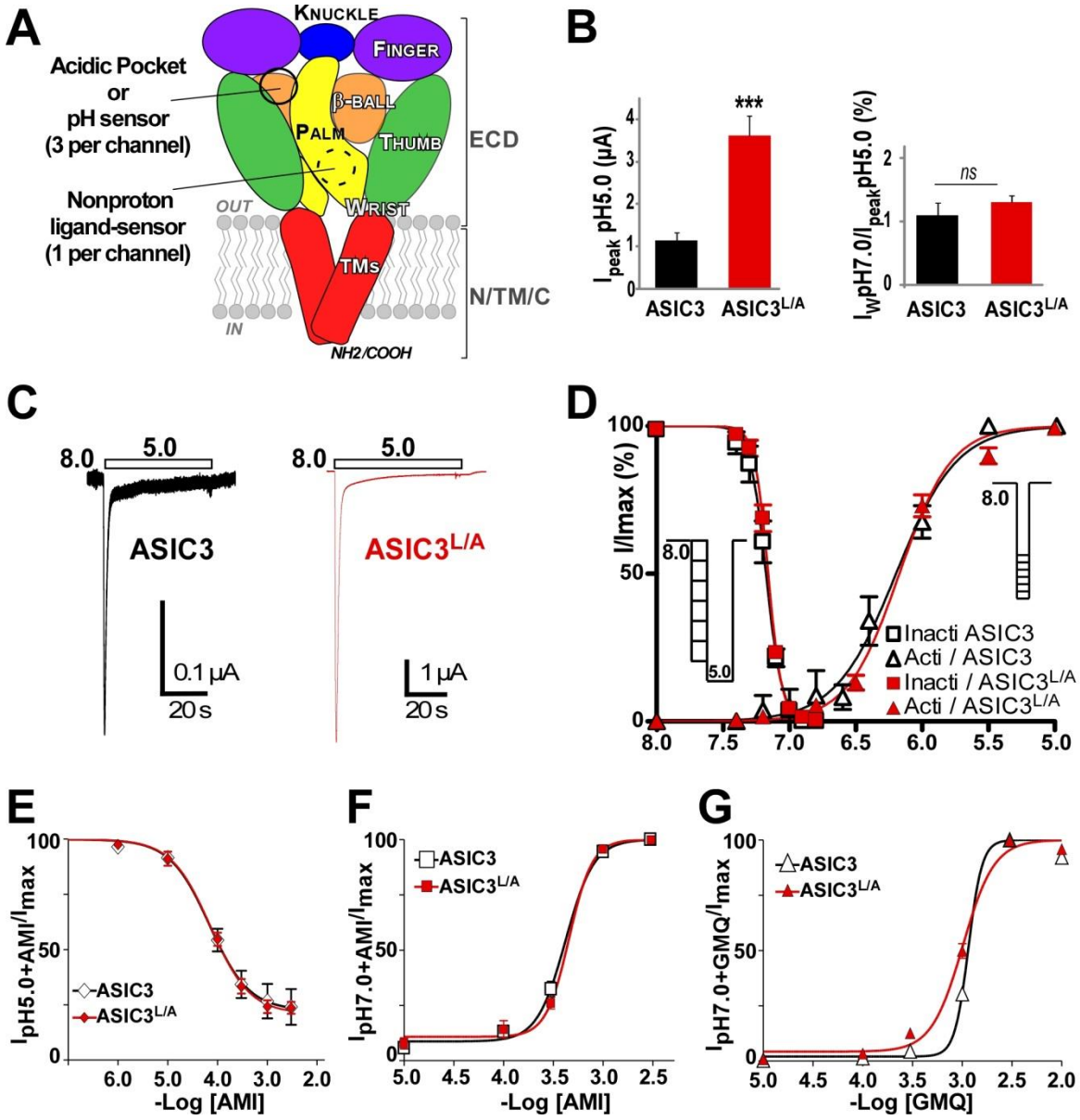

Supplementary Figure 1. ASIC3 wild-type and L529A point mutant (ASIC3$^{L/A}$) have the same functional properties. A) The different sub-domains in ASIC are schematically represented as described by Jasti et al. (Jasti et al., 2007), and only 2 subunits of the trimeric channel are shown for simplicity. Note that the ECD as defined here includes the very upper part of the transmembrane domains (TMs), i.e., the Wrist domain connecting the Thumb and the Palm domains with the TMs, to preserve proper coupling between the extracellular domain and the rest of the channel during pH-dependent gating. **B)** Statistical analysis of the peak current amplitudes associated with the ASIC3 and ASIC3$^{L/A}$ channels and induced by a drop in pH from 7.4 to 5.0 (top), and of the sustained window current at pH7.0 normalized to the peak current (bottom) (n=8-13; *** P<0.001, unpaired t-test). L529A corresponds to a mutation in a consensus motif for internalization closed to the end of the cytoplasmic carboxy-terminus (R…LV) that increased the peak current of ASIC3 by about 3-fold ($I_{peak\text{-}pH5.0}$= 1.14±0.20 and 3.62±0.47 µA for ASIC3 and ASIC3$^{L/A}$, respectively) without affecting the window current ($I_{sustained\text{-}pH7.0}/I_{peak\text{-}pH5.0}$= 1.09±0.20 % and 1.30±0.11 % for ASIC3 and ASIC3$^{L/A}$; P>0.05, unpaired t-test) and the others properties. **C)** Typical current traces showing the same characteristic biphasic current in ASIC3 and ASIC3$^{L/A}$. **D)** The pH-dependent curves of activation (triangle) and inactivation (square) for ASIC3 (black lines; n=5) and ASIC3$^{L/A}$

(red lines; n=6-8) are identical. Solid lines are fits of the mean values of each data point to a sigmoidal dose-response curve with variable slope. The pHs for half-maximal activation and inactivation are not significantly different between ASIC3 and ASIC3$^{L/A}$ (see values in Table 1). **E)** Amiloride inhibited in a similar way the ASIC3 and ASIC3$^{L/A}$ peak currents at pH5.0. Current amplitudes, normalized to amplitude in the absence of amiloride, are plotted as the inverse of a logarithmic function of amiloride concentration. The pIC_{50} values for ASIC3 and ASIC3$^{L/A}$ determined from the fit are $pIC_{50pH5.0+AMI}$=4.14±0.12 (n=6) and 4.16±0.06 (n=7), P>0.05*;* respectively. **F)** Amiloride similarly activated the ASIC3 and ASIC3$^{L/A}$ currents when applied at pH 7.0 ($pEC_{50pH7.0+AMI}$=3.37±0.02 (n=5) and 3.34±0.03 (n=5), P>0.05*;* respectively. **G)** Activation of the pH7.0-evoked ASIC3 and ASIC3$^{L/A}$ currents by GMQ are also not significantly different ($pEC_{50pH7.0+GMQ}$=2.99±0.02 (n=9) and 2.94±0.06 (n=8), P>0.05*;* respectively).

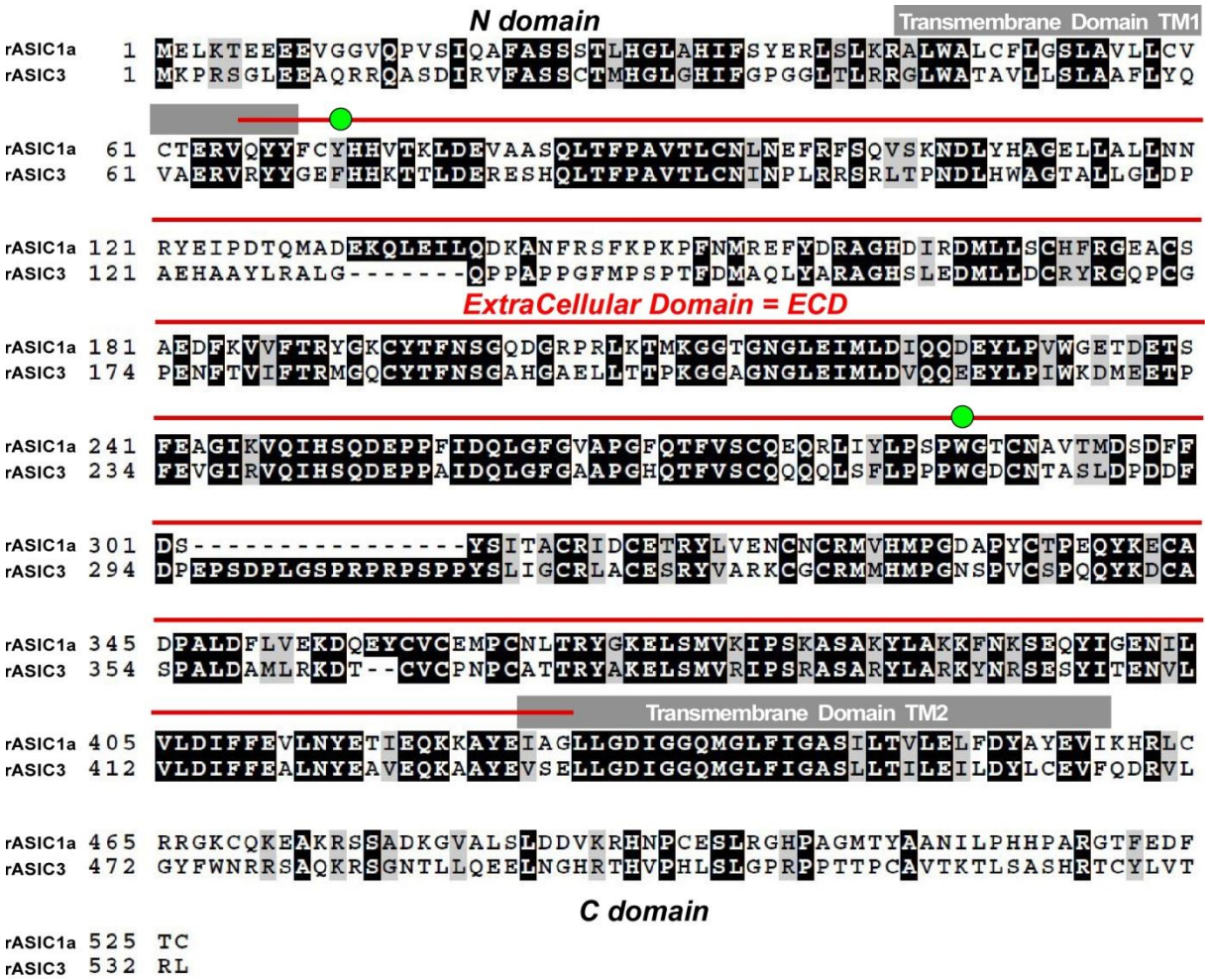

Supplementary Figure 2. Sequence alignement of rat ASIC1a and ASIC3. TM1 and TM2 indicate the position of transmembane domains 1 and 2. The cytosolic amino- and carboxy-terminal domains are noted N and C domains, respectively. The extracellular domain including the Wrist domain is shown in red and noted ECD. Tyr 71 and Trp 287 composing the contact between the Thumb domain and the TM1 domain are marked by green circles.

Reference

Jasti, J., Furukawa, H., Gonzales, E. B., Gouaux, E., 2007. Structure of acid-sensing ion channel 1 at 1.9 A resolution and low pH. Nature 449, 316-323. doi: 10.1038/nature06163.